Earth Planets Space, **60**, 387–390, 2008

The possibility of studying the lunar ionosphere with the SELENE radio science experiment

Takeshi Imamura[1], Koh-Ichiro Oyama[1], Takahiro Iwata[1], Yusuke Kono[2], Koji Matsumoto[2], Qinghui Liu[2], Hirotomo Noda[2], Yoshifumi Futaana[3], and Alexander Nabatov[4]

[1]*Institute of Space and Astronautical Science, Japan Aerospace Exploration Agency, Japan*
[2]*National Astronomical Observatory of Japan, Japan*
[3]*The Swedish Institute of Space Physics, Sweden*
[4]*Ukrainian Academy of Science, Ukraine*

(Received March 21, 2007; Revised October 5, 2007; Accepted October 5, 2007; Online published April 9, 2008)

The electron density profiles above the lunar surface will be observed by the radio occultation technique during the SELENE mission using the Vstar sub-satellite. Previous radio occultation observations have indicated the existence of an ionosphere with densities of up to 1000 cm^{-3} above the dayside lunar surface. The measured densities are difficult to explain theoretically when the removal of plasma by the solar wind is considered, and thus the generation mechanism of the lunar ionosphere is a major issue, with even the validity of previous observations still under debate. The SELENE radio science experiment will establish the morphology of the lunar ionosphere and will reveal its relationship with various physical conditions to provide possible clues to the mechanism.
Key words: Lunar ionosphere, SELENE, radio science.

1. Introduction

Charged particles that are present near the lunar surface are mostly the result of the interaction of the solar ultraviolet radiation and the solar wind with the lunar atmosphere and regolith (Stern, 1999). Very near the dayside surface a photoelectron sheath with a density of the order of 10^4 cm^{-3} and a height of a few hundred meters exists (Reasoner and Burke, 1972; Walbridge, 1973). Above this layer is an ionosphere, whose density is generally thought to be on the order of 1 cm^{-3} in the range from the surface to 100 km altitude (Stern, 1999). This ionosphere is probably produced by the photo-ionization of the tenuous neutral atmosphere (exosphere), which is composed mostly of Ar, Ne and He with a density of $\sim 10^5$ cm^{-3} on the dayside (Hodges *et al*., 1974). The process that may prevent the accumulation of newly produced ions near the lunar surface is the impingement of the solar wind magnetic field on the lunar surface, which induces an electric field that sweeps away ions (Johnson, 1971; Hodges *et al*., 1974). The timescale of this sweeping out process is given by the lunar radius divided by the solar wind speed, which is of the order of 1 s (Bauer, 1996), although this estimate may not apply to ions heavier than protons due to their large gyro radii. The high temperatures of photoelectrons compared to those of ions produce the Rosseland electric field, which also drags plasma away (Daily *et al*., 1977).

In contrast to these studies are several radio occultation experiments performed with radio stars, in which the radio sources showed large angular shifts when they were occulted by the dayside lunar limb (e.g., Elsmore, 1957; Andrew *et al*., 1964). These angular shifts can be explained by the refraction of radio waves in the lunar ionosphere, provided that the ionosphere has electron densities of $\sim$1000 cm^{-3} and a thickness of several tens of kilometers (Vyshlov and Savich, 1979). Dual-frequency radio occultation experiments conducted with the Soviet Luna 19 and 22 spacecraft also detected large electron densities near the dayside lunar surface (Vasilyev *et al*., 1974; Vyshlov, 1976; Vyshlov *et al*., 1976; Vyshlov and Savich, 1979). In radio occultation experiments, observed from a tracking station on the Earth, the spacecraft goes behind the lunar plasma layer and then behind the lunar disk, and reemerges in the reverse sequence. The plasma layer causes a time-dependent phase shift in the radio signal, from which the total electron content along the ray path can be retrieved. Under the assumption of spherical symmetry, Vyshlov (1976) obtained peak electron densities of 500–1000 cm^{-3} at heights of 5–10 km, with a gradual decrease at higher altitudes with a scale height of 10–30 km and also a decrease toward the surface. Daily *et al*. (1977) argued that these electron densities are extremely high and might be an artifact of the analytical technique. Bauer (1996) attributed them to the effect of the photoelectron sheath.

Savich (1976) argued that remnant magnetic fields might stand off the solar wind to allow the accumulation of plasma near the lunar surface. He suggested that if ions are trapped by the local magnetic field near the surface but the condition for mirroring is not fulfilled, then letting the neutral particle density be $\sim 10^6$ cm^{-3}, the ionization rate per particle be $\sim 10^{-6}$ s^{-1}, and the mean lifetime of ions be $\sim$400 s, the equilibrium ion density would be $\sim$400 cm^{-3}. He also suggested that if particle reflection does occur, the ion life-

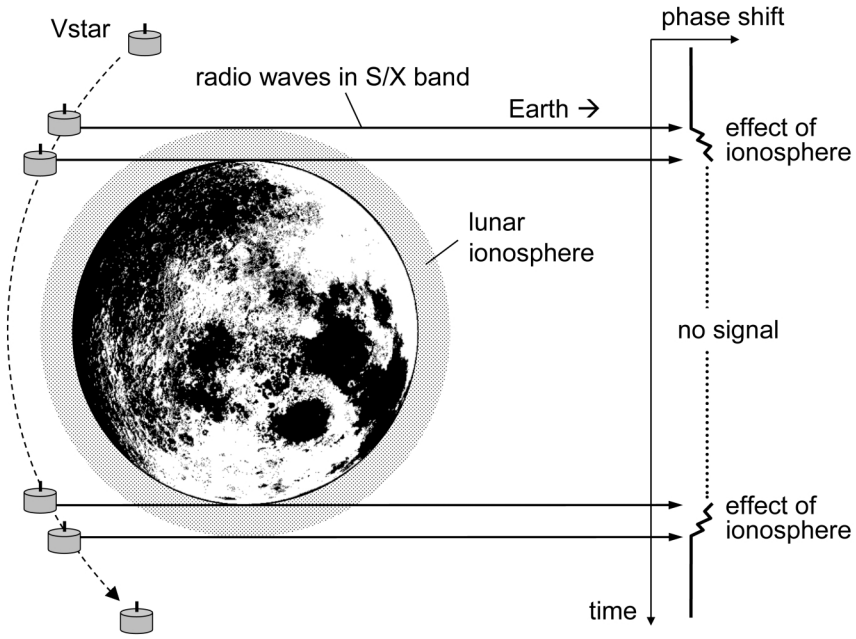

Fig. 1. Schematic of the radio science experiment using Vstar sub-satellite in the SELENE mission.

time would then be limited by the curvature drift time scale of ∼8000 s and the coefficient of trapping of ∼0.2, and the equilibrium ion density would reach ∼1600 cm^{-3}. Remnant magnetic fields have been found on the lunar surface by the Apollo and Lunar Prospector missions (Lin *et al.*, 1988, 1998); the field intensities reaching ∼300 nT on spatial scales up to 1000 km. Numerical experiments demonstrated that such local magnetic fields can stand off the solar wind to create mini-magnetosphere systems near the surface (Harnett and Winglee, 2000). Futaana *et al.* (2003) used Nozomi ion spectrometer data and found protons that may have been reflected by a mini-magnetosphere system.

Other explanations are also feasible. Daily *et al.* (1977) argued that the release of abundant neutral Ar from the lunar surface near the sunrise terminator would enhance ionization; the Luna 19 and 22 occultation measurements on the dayside of the moon were all made near the sunrise terminator. Stubbs *et al.* (2006) suggested that charged dust grains near the lunar surface could be accelerated upward by the near-surface electric field and reach high altitudes, thereby explaining the scattering of the sunlight above the horizon at the terminators observed by the Apollo landers and astronauts in orbit. Such charged dust clouds might be accompanied by substantial numbers of electrons.

In summary, the possible existence of the ionized layer above the lunar surface might be attributed to the effect of the remnant magnetic field, to certain processes that enhance the neutral gas concentration, or to charged dust grains that are lifted up by the near-surface electric field. The radio science (RS) experiments in the SELENE (SELenological and Engineering Explorer) mission will provide opportunities to systematically study this ionized layer to examine its existence and to understand the generation mechanism (Oyama *et al.*, 2002; Nabatov *et al.*, 2003). The following sections describe the method of observation.

2. Observation Sequence

The SELENE spacecraft will be launched in the summer of 2007 and inserted into a moon-encircling orbit after spending a few weeks in a phasing orbit around the Earth. Two sub-satellites, Rstar and Vstar, will be separated from the main orbiter after the lunar orbit insertion. Both Rstar and Vstar carry radio sources for the VLBI experiments, and Rstar also relays 4-way communication between the main orbiter and the ground station. We will utilize the coherent S-band (2.218 GHz) and X-band (8.456 GHz) signals transmitted from Vstar for the radio science investigation of the lunar ionosphere (Fig. 1).

Vstar is a spinning spacecraft with a mass of 45 kg and a size of $1\times1\times0.65$ m. The spin axis is roughly perpendicular to the equatorial plane, and an omni antenna is oriented along this axis, providing a continuous link with the ground station. The attitude of the spacecraft is expected to be stable for over a year. The spacecraft will be put into a polar orbit with a period of ∼153 minutes, a periapsis altitude of 100 km and an apoapsis altitude of 800 km. Because of the synchronization of the rotation with the revolution of the moon, only the area in the vicinity of the lunar limb as seen from Earth is accessible by radio occultation. The size of the accessible area is determined by the liberation of the moon and will amount to ∼10% of the lunar surface in total. The transmission power will be 0.1 W and the transmitted waves will not be modulated. The frequency of the transmitted wave will change with temperature by ∼300 Hz K^{-1} in the S-band and by ∼1000 Hz K^{-1} in the X-band due to the change in output frequency of the common frequency source. Although this oscillator is not very stable, the dual-frequency method enables us to remove the influence of this frequency fluctuation as will be described later.

The S- and X-band signals transmitted by Vstar will be received by the 64-m antenna at the Usuda Deep Space Center (UDSC) in Japan. The received signals will be

converted to ∼20 kHz by an open-loop heterodyne system stabilized by a hydrogen maser (Allan deviation $< 3\times10^{-13}$ for 1 sec, $< 3\times10^{-15}$ for 1000 sec), followed by digitization with a sampling rate of 80 kHz. Signals will be recorded for 10–20 minutes just before each ingress occultation and just after each egress occultation. Given the typical transverse velocity of the ray path of ∼1 km sec^{-1} in the course of the orbital motion of Vstar, the time needed to probe the whole lunar ionosphere of ∼50 km thickness is ∼1 minute. The opportunities of observations will be determined not only by orbital dynamics of the satellites but also by the schedule of other tracking operations at UDSC; the total number of observations during the 1-year nominal mission will be about 50. Further observations are planned for the extended mission period, depending on the condition of the spacecraft.

3. Method of Analysis

Although the onboard oscillator is not very stable, taking a linear combination of the phases in the two coherent bands will enable us to distinguish the plasma contributions from the fluctuation in the oscillator output frequency (e.g., Oyama *et al.*, 2001). The frequency fluctuations in the two bands that are generated from a common oscillator will be synchronized and have magnitudes that are proportional to their nominal frequencies. The difference in the temperature fluctuations at the onboard phase-locked loops for the two bands may cause errors that cannot be removed by the linear combination; however, such fluctuations are expected to have time scales longer than 1000 s and will not distort the measurements which have much shorter time scales.

The time-dependent phase shift in the S-band, $\Delta\phi_{\rm S}(t)$, and that in the X-band, $\Delta\phi_{\rm X}(t)$, which are measured with respect to the phase variation for the plasma-free case based on the orbital information, can be expressed as

$$\Delta\phi_{\rm S}(t) = \frac{\alpha}{cf_{\rm S}}N_e(t) + \beta f_{\rm S}, \tag{1}$$

$$\Delta\phi_{\rm X}(t) = \frac{\alpha}{cf_{\rm X}}N_e(t) + \beta f_{\rm X}, \tag{2}$$

where $\alpha = e^2/8\pi^2\varepsilon_0 m_e \sim 40.3$ m^3 s^{-2} with e, ε_0 and m_e being the elementary charge, dielectric constant in vacuum and electron mass, respectively, c the speed of light in m s^{-1}, $f_{\rm S}$ and $f_{\rm X}$ the nominal frequencies of the S- and X-band, respectively, $N_e(t)$ the time-dependent electron column density along the ray path in m^{-2}, and β the sum of proportionality constants. These phases are expressed in units of cycles. The first terms on the right-hand-sides of (1) and (2) represent the contribution from the plasma along the ray path, and the second terms represent the sum of several effects, i.e., the fluctuations in the oscillator output frequency, the influence of the terrestrial neutral atmosphere the refractive index of which is independent of the frequency, and the effects of the uncertainties in orbital motions on the Doppler shift. The differential phase $\delta\phi(t)$ is defined to be a linear combination of (1) and (2):

$$\delta\phi(t) = \Delta\phi_{\rm S}(t) - \frac{f_{\rm S}}{f_{\rm X}}\Delta\phi_{\rm X}(t) = \frac{\alpha}{c}f_{\rm S}\left(\frac{1}{f_{\rm S}^2} - \frac{1}{f_{\rm X}^2}\right)\cdot N_e(t). \tag{3}$$

This relationship will enable us to derive $N_e(t)$ from the observed phases without being disturbed by fluctuations in the oscillator output frequency.

In the region where the contribution of the lunar ionosphere is virtually absent, i.e. at altitudes above 50 km, a gradual variation caused by the terrestrial ionosphere will be observed. This variation will be extrapolated into the near-moon portion and subtracted from the observed one, thereby eliminating the influence of the terrestrial ionosphere to some extent. The resultant $N_e(t)$ will be converted to a function of the altitude above the surface using orbital information. The vertical profile of electron density will be calculated assuming spherical symmetry of the ionosphere.

The $\Delta\phi_{\rm S}(t)$ and $\Delta\phi_{\rm X}(t)$ will be retrieved from the recorded signal in the following manner (Imamura *et al.*, 2005). First the approximate carrier frequency will be determined for successive time blocks by fitting a theoretical signal spectrum to the discrete Fourier transform of the voltage variation in successive blocks (Lipa and Tyler, 1979). Next polynomial functions will be fitted to the frequency time series above, and the resultant frequency variation corresponding to the polynomial will be subtracted from the original signal by heterodyning. In the course of the data reduction, the signal will be bandpass-filtered repeatedly to increase the signal-to-noise ratio, and at the same time decimated. This filtering scheme automatically converts the data to a complex representation, in which each datum comprises both the amplitude and phase of the signal. The low-noise signal, after filtering, will yield the phase by removing cycle slips via the phase unwrapping procedure (Mizuno *et al.*, 1992). The sum of the phase variation in this final product and the phase variation that has been subtracted via heterodyning in the course of the processing will give the total phase shift.

4. Accuracy of Measurement

The required accuracy for N_e is taken to be $\sigma_N = 6\times10^{13}$ m^{-2}, which is about 20% of the column density of $\sim 3\times10^{14}$ m^{-2} observed by Luna 19 and 22 (Vyshlov and Savich, 1979). Then, from (3), the required accuracy for $\delta\phi$ is $\sigma_{\delta\phi} \sim 0.021$ radian, giving the required accuracy for $\Delta\phi_{\rm S}$ of $\sigma_{\delta\phi}/\sqrt{2} \sim 0.015$ radian and that for $\Delta\phi_{\rm X}$ of $(f_{\rm X}/f_{\rm S})\sigma_{\delta\phi}/\sqrt{2} \sim 0.054$ radian. Letting the required vertical resolution be 1 km, the temporal resolution of the measurement should be better than 1 s, giving the required bandwidth of $B = 1$ Hz. Since the accuracy in phase $\Delta\phi$ is related to the carrier-to-noise density ratio (C/N$_0$) of the received signal, CNR, by $\Delta\phi = (2{\rm CNR}/B)^{-0.5}$, the required CNR for the S- and X-band can be calculated to be ∼34 dB Hz and ∼22 dB Hz, respectively. These values are achievable according to the link budget analysis for the mission.

The most serious source of error is the density fluctuation in the terrestrial ionosphere. Noguchi *et al.* (2001) studied the root-mean-square (rms) of the total electron content (TEC) fluctuation with periods of 1–10 minutes over UDSC, as a function of season and local time, using the GPS (Global Positioning System) TEC data with a sampling interval of 30 s. They showed that the hourly-averaged rms is of the order of 10^{14} m^{-2} which is a similar value to

the lunar electron content integrated along the ray path, except for the nighttime in summer and the daytime in winter where the rms reaches $\sim 10^{15}$ m^{-2}. They also suggested that nighttime in winter is the most suitable time for occultation measurements. The probability of detection cannot be estimated based on this study, however, due to the coarse sampling in the GPS TEC data compared to the timescale of the lunar occultation measurements. Recently GPS TEC data have become available for sampling every second; using such data the contribution of the terrestrial ionosphere will be monitored and subtracted from radio occultation results except under highly disturbed conditions.

5. Conclusions

Radio occultation observations conducted in the 1960s and 1970s using natural radio sources and spacecraft indicated the existence of a lunar ionosphere with densities of $\sim$1000 cm^{-3} and a thickness of several tens of kilometers near the dayside lunar surface. This ionospheric density is difficult to explain using existing theories when the removal of plasma by the solar wind is considered; the predicted densities are on the order of 1 cm^{-3}. The roles of remnant magnetic field, the sporadic supply of neutral gases and suspended dust have been proposed; however, the limited observational data do not allow close investigations of specific processes that may increase electron density. Even the reliability of the previous observations is still under debate. The systematic measurements proposed for the SELENE radio science experiment using the Vstar sub-satellite will establish the morphology of the lunar ionosphere and reveal its dependence on the remnant magnetic field, solar incident angle, and solar wind conditions, thereby providing clues to the generation mechanism of the ionosphere.

Instruments onboard the SELENE main orbiter will provide additional information to aid the interpretation of the radio science results. The Lunar Magnetometer (LMAG) will map the remnant magnetic field and also monitor the magnetic field of the solar wind and the terrestrial magnetosphere near the moon. The Plasma energy Angle and Composition Experiment (PACE) will observe the energy distributions of electrons and ions directly. The Charged Particle Spectrometer (CPS) will observe local gas ejections, which may lead to an increase in ionization, and will also monitors incident energetic particles, which sputter charged particles from the lunar surface. The combination of these measurements together with radio science investigation should result in an unprecedented detailed analysis of the lunar electromagnetic environment.

Acknowledgments. We would like to acknowledge Z. Yamamoto, all members of the SELENE project team and the staff of UDSC for supporting the experiment. This experiment would not have become possible without the assistance of S. Ohashi, M. Sugiura and other engineers of NEC TOSHIBA Space Systems, Ltd.

References

Andrew, B. H., N. J. B. A. Branson, and D. Wills, Radio observations of the Crab nebula during a lunar occultation, *Nature*, **203**, 171–173, 1964.

Bauer, S. J., Limits to a lunar ionosphere, *Anzeiger Abt. II*, **133**, 17–21, 1996.

Daily, W. D., W. A. Barker, C. W. Parkin, M. Clark, and P. Dyal, Ionosphere and atmosphere of the moon in the geomagnetic tail, *J. Geophys. Res.*, **82**, 5441–5451, 1977.

Elsmore, B., Radio observations of the lunar atmosphere, *Phil. Mag.*, **2**, 1040–1046, 1957.

Futaana, Y., S. Machida, Y. Saito, A. Matsuoka, and H. Hayakawa, Moon-related nonthermal ions observed by NOZOMI—species, sources, and generation mechanisms, *J. Geophys. Res.*, **108**, 1025, doi:10.1029/2002JA009366, 2003.

Harnett, E. and R. Winglee, Two dimensional MHD simulation of the solar wind interaction with magnetic field anomalies on the surface of the Moon, *J. Geophys. Res.*, **105**, 24997–25007, 2000.

Hodges, R. R., Jr., J. H. Hoffman, and F. S. Johnson, The lunar atmosphere, *Icarus*, **21**, 415–426, 1974.

Imamura, T., K. Noguchi, A. Nabatov, K.-I. Oyama, Z. Yamamoto, and M. Tokumaru, Phase scintillation observation during coronal sounding experiments with NOZOMI spacecraft, *Astron. Astrophys.*, **439**, 1165–1169, 2005.

Johnson, F. S., Lunar atmosphere, *Rev. Geophys. And Space Phys.*, **9**, 813–823, 1971.

Lin, R. P., K. A. Anderson, and L. L. Hood, Lunar surface magnetic field concentrations antipodal to young large impact basins, *Icarus*, **74**, 529–541, 1988.

Lin, R. P., D. L. Mitchell, D. W. Curtis, K. A. Anderson, C. W. Carlson, J. McFadden, M. H. Acuna, L. L. Hood, and A. Binder, Lunar Surface Magnetic Fields and Their Interaction with the Solar Wind: Results from Lunar Prospector, *Science*, **281**, 1480–1484, 1998.

Lipa, B. and L. Tyler, Statistical and computational uncertainties in atmospheric profiles from radio occultation: Mariner 10 at Venus, *Icarus*, **39**, 192–208, 1979.

Mizuno, E., N. Kawashima, T. Takano, and P. A. Rosen, Voyager radio science: observations and analysis of Neptune's atmosphere, *IEICE Trans. Commun.*, **E75-B**, 665–672, 1992.

Nabatov, A. S., T. Imamura, N. A. Savich, K.-I. Oyama, and K. Noguchi, Detectability of lunar plasma clouds from Selene radio occultations, *Adv. Space Res.*, **31**(11), 2369–2375, 2003.

Noguchi, K., T. Imamura, K.-I. Oyama, and A. Saito, Application of the GPS network to estimate the effect of the terrestrial ionosphere on the radio occultation measurements of planetary ionospheres, *Radio Sci.*, **36**, 1607–1614, 2001.

Oyama, K.-I., A. Nabatov, N. Savich, Z. Yamamoto, T. Imamura, T. Ichikawa, and K. Noguchi, First test of the Nozomi radio science system in actual space flight, *Adv. Space Res.*, **27**(11), 1847–1850, 2001.

Oyama, K.-I., A. Nabatov, N. Savich, T. Imamura, Z. Yamamoto, and K. Noguchi, Cislunar plasma exploration with the Selene radio science system, *Adv. Space Res.*, **30**(8), 1915–1919, 2002.

Reasoner, D. L. and W. J. Burke, Characteristics of the lunar photoelectron layer in the geomagnetic tail, *J. Geophys. Res.*, **77**, 6671–6687, 1972.

Savich, N. A., Cislunar plasma model, *Space Res.*, **16**, 941–943, 1976.

Stern, S. A., The lunar atmosphere: History, status, current problems, and context, *Rev. Geophys.*, **37**, 453–492, 1999.

Stubbs, T. J., R. R. Vondrak, and W. M. Farrell, A dynamic fountain model for lunar dust, *Adv. Space Res.*, **37**, 59–66, 2006.

Vasilyev, M. B., V. A. Vinogradov, A. S. Vyshlov, O. G. Ivanovskii, M. A. Kolosov, N. A. Savich, V. A. Samovol, L. N. Samoznaev, A. I. Sidorenko, A. I. Sheikhet, and D. Ya. Shtern, Radio transparency of circumlunar space using the Luna-19 station, *Cosmic Res.*, **12**, 102–107, 1974.

Vyshlov, A. S., Preliminary results of circumlunar plasma research by the Luna 22. spacecraft, *Space Res.*, **16**, 945–949, 1976.

Vyshlov, A. S. and N. A. Savich, Observations of radio source occultations by the moon and the nature of the plasma near the moon, *Cosmic Res.*, **16**, 450–454, 1979.

Vyshlov, A. S., N. A. Savich, M. B. Vasilyev, L. N. Samoznaev, A. I. Sidorenko, and D. Y. Shtern, Some results of cislunar plasma research, *Solar-Wind Interaction with the Planets Mercury, Venus, and Mars, NASA*, 81–85, 1976.

Walbridge, E., Lunar photoelectron layer, *J. Geophys. Res.*, **78**, 3668–3687, 1973.

T. Imamura (e-mail: ima@isas.jaxa.jp), K.-I. Oyama, T. Iwata, Y. Kono, K. Matsumoto, Q. Liu, H. Noda, Y. Futaana, and A. Nabatov